JULY 12–16
2020 VIRTUAL
JOINT AAPM | COMP MEETING
EASTERN TIME [GMT-4]

Evaluating the Clinical Utility of Cherenkov Imaging in Radiotherapy

R HACHADORIAN 1*, D. ALEXANDER, I TENDLER, B. POGUE., L. JARVIS.
1 Thayer School of Engineering, Dartmouth College, Hanover, NH USA
2 DoseOptics LLC, Lebanon, NH USA
3 Geisel School of Medicine, Hanover, NH USA
4 Norris Cotton Cancer Center, Dartmouth-Hitchcock Medical Center, Lebanon, NH USA

THAYER SCHOOL OF ENGINEERING AT DARTMOUTH
CENTER FOR IMAGING MEDICINE AT DARTMOUTH

INTRODUCTION

The value of Cherenkov imaging as an on-patient, real-time treatment delivery verification system was examined in a 64 patient-cohort during routine radiation treatments in a single center study. Cherenkov cameras were mounted in treatment rooms and used to image patients during their standard radiotherapy regimen, predominantly for whole breast, total skin, or head and neck cancers. For most patients, multiple fractions were imaged with some involving bolus or scintillator patches on the skin. Measures of repeatability were calculated with a mean distance to conformity (MDC) for breast irradiation images.

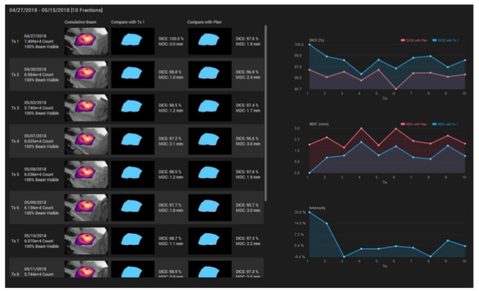

FIGURE 1: Once a patient is consented for the study, all fractions of treatment are recorded. All the frames from each treatment are summed into cumulative images, then binarized and assessed for shape consistency. Future work includes correcting for not just beam shape, but also for dose at the surface.

AIM

After completing over 200 fractions of Cherenkov imaging over regularly scheduled and prescribed radiation treatments, including over 100 breast fractions, the largest Cherenkov imaged patient cohort available, a thorough evaluation of the overall clinical utility of Cherenkov imaging was carried out to share the ways in which it has proved to be clinically useful over the last several years. This assessment also helped the authors to plan and direct future work.

METHODS

Cherenkov cameras were mounted in treatment rooms and used to image patients during their standard radiotherapy regimen, predominantly for whole breast, total skin, or head and neck cancers. For most patients, multiple fractions were imaged with some involving bolus or scintillator patches on the skin.

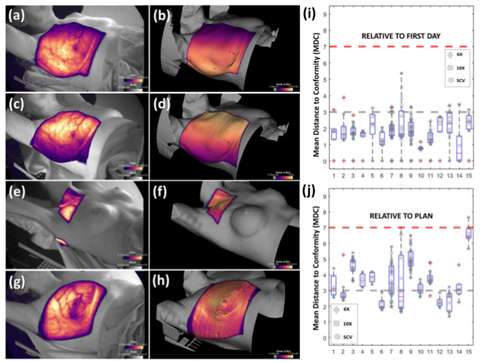

FIGURE 2: A sample of a right posterior oblique beam (RPO) Cherenkov image for a patient is shown in (a), which matches the intensity map from the treatment plan (b). The same is shown for the LAO (left anterior oblique) beam (c) which also includes a couch kick, along with its respective cumulative treatment plan image (d). These individual beams illustrate the dose gradient over the surface of the patient, with higher intensity on the entrance side and lower intensity on the exit side, over a gradient. One example of a supraclavicular field is shown in the Cherenkov image (e) and dose image exported from the treatment plan (f). For (another patient, the cumulative treatment of both LAO and RPO beams Cherenkov image (g) is shown matching the cumulative treatment dose image (h). In (i), the mean distance to conformity MDC) relative to the first recorded treatment day is plotted for all breast patient images, and in (j) this is replotted relative to the treatment plan dose outline as a reference. A dashed gray line indicates where treatment fractions fall within a 3 mm MDC agreement and a red dashed line indicates a 7 mm MDC agreement.

RESULTS

In breast treatments, Cherenkov images identified fractions when treatment delivery resulted in dose on the contralateral breast, the arm, or the chin, and found non-ideal bolus positioning. In sarcoma treatments, safe positioning of the contralateral leg was monitored. For all 199 imaged breast treatment fields, the inter-fraction MDC was within 7 mm as compared to the first day of treatment (with only 7.5% of treatments exceeding 3 mm), and all but one fell within 7 mm relative to the treatment plan. The value of imaging dose through clear bolus or quantifying surface dose with scintillator dots was examined, Cherenkov imaging also was able to assess field match lines in cerebral-spinal irradiation and breast irradiation with nodes. Similarly, treatment imaging of complex head and neck plans was confirmed.

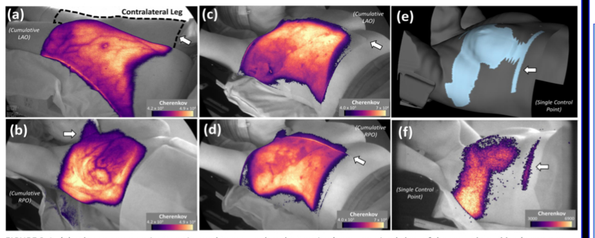

FIGURE 3: In (a), a leg sarcoma patient was imaged to ensure that the treating beam remained clear of the contralateral leg (a common focus point in the treatment of extremities such as legs). High tangents are another common focus point, shown in (b), where it can be seen if the patient were to move his/her head or chin, which has many degrees of freedom and lacks immobilization. When treating a patient with mastectomy using bolus, accommodating the large field sizes can be difficult, which is shown comparing (c), where the LAO field was successfully covered with bolus, whereas the RPO field (d) was not on the medial side. In a less common case where an MLC was accidentally left open during planning (e), the Cherenkov image (f) shows this incident very clearly:

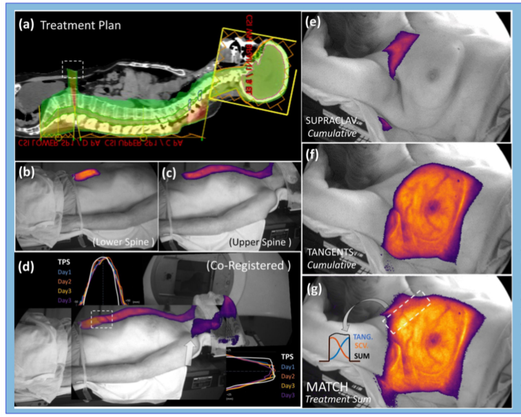

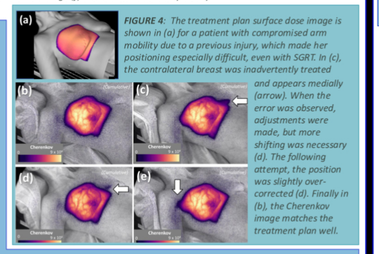

FIGURE 4: The treatment plan surface dose image is shown in (a) for a patient with compromised arm mobility due to a previous injury, which made her positioning especially difficult, even with SGRT. In (c), the contralateral breast was inadvertently treated and appears medially (arrow). When the error was observed, adjustments were made, but more shifting was necessary (d). The following attempt, the position was slightly over-corrected (d). Finally in (b), the Cherenkov image matches the treatment plan well.

FIGURE 5: A treatment plan for cerebral-spinal irradiation (CSI) is shown (a), which was characterized by four fields and three isocenters: a right and left lateral whole brain field, an upper spine field and a lower spine field. A technique for stitching together the Cherenkov treatment images was developed by first isolating the lower spine field individually in (b) and upper spine in (c). The result in (d) shows the sum, with biological fiducials used to register the background and Cherenkov images together. Image (d) shows profiles comparing days 1 through 4 of lower and upper spine junction areas, as compared what was seen in the treatment plan. In (e), the supraclavicular cumulative fields treating the axial nodes of a patient are shown. In (f), the four tangent beam images (LAO/RPO 6X/10X) summed together are shown, and added with the supraclavicular field in (g). The match region has a bounding box that isolates the profile intersection region, such that the meeting of the two beams can be analyzed.

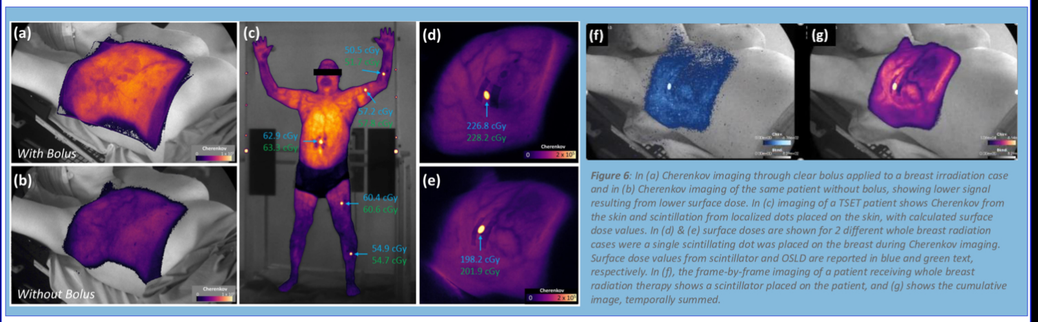

Figure 6: In (a) Cherenkov imaging through clear bolus applied to a breast irradiation case and in (b) Cherenkov imaging of the same patient without bolus, showing lower signal resulting from lower surface dose. In (c) imaging of a TSET patient shows Cherenkov from the skin and scintillation from localized dots placed on the skin, with calculated surface dose values. In (d) & (e) surface doses are shown for 2 different whole breast radiation cases were a single scintillating dot was placed on the breast during Cherenkov imaging. Surface dose values from scintillator and OSLD are reported in blue and green text, respectively. In (f), the frame-by-frame imaging of a patient receiving whole breast radiation therapy shows a scintillator placed on the patient, and (g) shows the cumulative image, temporally summed.

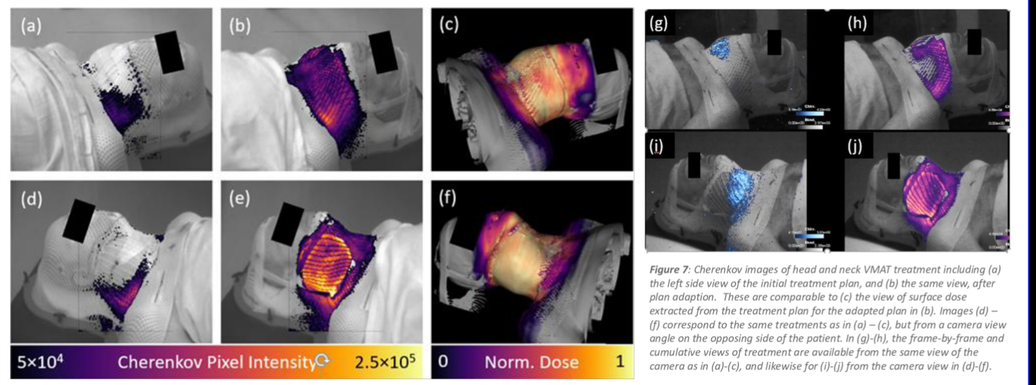

Figure 7: Cherenkov images of head and neck VMAT treatment including (a) the left side view of the initial treatment plan, and (b) the same view, after plan adaptation. These are comparable to (c) the view of surface dose extracted from the treatment plan for the adapted plan in (b). Images (d) – (f) correspond to the same treatments as in (a) – (c), but from a camera view angle on the opposing side of the patient. In (g)-(h), the frame-by-frame and cumulative views of treatment are available from the same view of the camera as in (a)-(c), and likewise for (i)-(j) from the camera view in (d)-(f).

CONCLUSIONS / FUTURE WORK

Daily fractionated radiotherapy can be imaged with Cherenkov emission, and the cumulative images provide maps of surface dose delivery that can be used for incident discovery or continuous improvement in technique delivery. In this 64-patient cohort, we discovered no major clinical incidents, but did discover approximately six incidents that could lead to better technique in the future, and confirmed the safe treatment delivery to three patients which were previously cause for concern. Taken as a pilot test, this indicates potential value of Cherenkov imaging as a tool to visualize treatment and for possible daily discovery of areas for technique improvement.

Other future work includes the representation of Cherenkov light, translated into dose, directly on a 3D rendering of the patient generated from the CT scan. Additionally, it has been proposed that always-on imaging could mitigate out dependence on the clinician to record and monitor the patient. These techniques are also saved for future patient imaging.

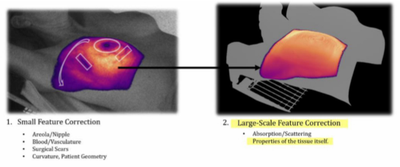

FIGURE 8: Some future work includes the correction of the tissue optical properties that vary amongst patients, such that the Cherenkov light can be translated into dose. This can be achieved once small-scale features and large-scale tissue differences in scatter and absorption can be corrected out. The plot animation then shows how this leads to Cherenkov to dose nonlinearity, and how the relationship should change once appropriate corrections have been achieved.

REFERENCES

[1] Sheldley, K.D., R.M. Eastman, and R.J. Stabile, *Observations of visual sensations produced by Cherenkov radiation from high-energy electrons.* Int J Radiat Oncol Biol Phys, **17**(3): p. 685-90(1989).
[2] Newman, F., M. Asadi-Zeydabadi, V.D. Duraraj, M. Ding, K. Stahr, and B.K.Kavanagh, *Visual sensations during megavoltage radiotherapy to the orbit attributable to Cherenkov radiation.* Med Phys, **35**(1): p. 77-80(2008).
[3] Jarvis, L.A., R. Zhang, D.J. Gladstone, S. Jiang, W. Hitchcock, O.D. Friedman, A.K. Glaser, M. Jermyn, and B.W. Pogue, *Cherenkov video imaging allows for the first visualization of radiation therapy in real time.* Int J Radiat Oncol Biol Phys, **89**(3): p. 615-22(2014).
[4] Andreozzi, J.M., R. Zhang, A.K. Glaser, L.A. Jarvis, B.W. Pogue, and D.J. Gladstone, *Camera selection for real-time in vivo radiation treatment verification systems using Cherenkov imaging.* Med Phys, **42**(2): p. 994-1004 (2015).
[5] Cerenkov, P., *Visible radiation produced by electrons moving in a medium with velocities exceeding that of light.* Physical Review, **52**(4): p. 378 (1937).
[6] Blumenthal, D.T., B.W. Corn, and N. Ishiyau, *Flashes of light-radiation therapy to the brain.* Radiother Oncol, **126**(2): p. 331-3(2015).
[7] Fahrenius, B., A. Ceballos, S. Turkcan, D.S. Kapp, and G. Prato, *Seeing the invisible: direct visualization of therapeutic radiation beams using air scintillation.* Med Phys, **41**(1): p. 010702(2014).
[8] Black, P.J., C. Velten, Y.F. Wang, Y.H. Na, and C.S. Wuu, *An investigation of clinical treatment field delivery verification using cherenkov imaging: IMRT positioning shifts and field matching.* Med Phys, **46**(1): p. 302-317 (2019).
[9] Kosunalp, Y., R. Zhang, G. Hayes, G. Webster, S. Mason, S. Green, B. Pogue, and H. Dehghani, *Real-time Cherenkov emission portal imaging during CyberKnife(R) radiotherapy.* Phys Med Biol, **60**(22): p. N419-25 (2015).
[10] Zhang, R., J.M. Andreozzi, D.J. Gladstone, W.L. Hitchcock, A.K. Glaser, S. Jiang, B.W. Pogue, and L.A. Jarvis, *Cherenkov-log based patient positioning validation and movement tracking during post-lumpectomy whole breast radiation therapy.* Phys Med Biol, **60**(3): p. 1131-41(2015).
[11] Mao, T., P. Bruza, B.W. Pogue, M. Jermyn, V. Krishnaswamy, W. Ware, F. Rafla, D.J. Gladstone, and B.B. Williams, *Cherenkov imaging for linac beam shape analysis as a remote electronic quality assessment verification tool.* Med Phys, **46**(2): p. 811-821 (2019).
[12] *AAPM Medical Physics Practice Guideline 5.a.: Commissioning and QA of Treatment Planning Dose Calculations – Megavoltage Photon and Electron Beams.* J Appl Clin Med Phys, **17**(1): p. 457(2016).
[13] Ford, E. and J. Deye, *Current Instrumentation and Technologies in Modern Radiotherapy Research Opportunities and Challenges.* Semin Radiat Oncol, **26**(4): p. 349-55 (2016).
[14] Hachadorian, R., P. Bruza, M. Jermyn, A. Mazhar, D. Cuccia, L. Jarvis, D. Gladstone, and B. Pogue, *Correcting Cherenkov-light attenuation in tissue using spatial frequency-domain imaging for quantitative surface dosimetry during whole breast radiation therapy.* J Biomed Opt, **24**(7): p. 1-12 (2019).
[15] Zhang, R., M. Petroccia, A. Mesty, T. Mao, Y. Zhu, P. Bruza, B.W. Pogue, J.P. Plastaras, L. Dong, and T.C. Zhu, *Cherenkov imaging for total skin electron therapy (TSET).* Med Phys, **47**(1): p. 203-212 (2020).
[16] Zhang, R., D.J. Gladstone, L.A. Jarvis, R.R. Strangeland, P. Jack Hoopes, D.D. Fiedler, A.K. Glaser, and B.W. Pogue, *Real-time in vivo Cherenkoscopy imaging during external beam radiation therapy.* J Biomed Opt, **18**(11): p. 116504(2013).
[17] Michalski, J.M., E.E. Klein, and R. Gerber, *Method to plan, administer, and verify supine craniospinal irradiation.* J Appl Clin Med Phys, **3**(4): p. 310-6 (2002).
[18] McMahon, R.L., N.A. Lerner, and G.J. Wu, *An image-guided technique for planning and verification of supine craniospinal irradiation.* J Appl Clin Med Phys, **12**(2): p. 3310 (2011).
[19] Chan, Z., A.G. Agnihotrah, L.D. Wilson, and R. Nath, *Matching the dosimetry characteristics of a dual-field Stanford technique to a customized single-field Stanford technique for total skin electron therapy.* Int J Radiat Oncol Biol Phys, **59**(3): p. 872-85 (2004).
[20] Gamble, L.M., T.J. Farrell, G.W. Jones, and J.E. Hayward, *Composite depth dose measurement for total skin electron (TSE) treatments using radiochromic film.* Phys Med Biol, **40**(7): p. 891-8 (2000).
[21] Adamson, J.D., T. Cooney, F. Damrahi, A. Stalnecker, D. Georges, F.F. Yin, and J. Kirkpatrick, *Characterization of Water Clear Polymeric Gels for Use as Radiotherapy Bolus.* Technol Cancer Res Treat: p. 1533034617715579 (2017).
[22] McMahon, R. L., Lerner, N. A., & Wu, Q. J. (2011). An image-guided technique for planning and verification of supine craniospinal irradiation. *Journal of applied clinical medical physics*, *12*(2), 184-190.
[23] Bruza, P., Gollub, S. L., Andreozzi, J. M., Tendler, I. I., Williams, B. B., Jarvis, L. A., ... & Pogue, B. W. (2018). Time-gated scintillator imaging for real-time optical surface dosimetry in total skin electron therapy. *Physics in Medicine & Biology*, *63*(18), 185006.
[24] Hachadorian, R. L., Jarvis, L. A., Gladstone, D. J., Jermyn, M., Bruza, P., & Pogue, B. W. (2019). Using Cherenkov imaging to Assess Field Overlap in Cranial-Spinal Irradiation (CSI). *International Journal of Radiation Oncology• Biology• Physics*, *105*(1), E729-E730.
[25] Tendler, I., P. Bruza, J. Andreozzi, M. Jermyn, B. Williams, L. Jarvis, B. Pogue, and D. Gladstone, *Rapid Multi-Site Remote Surface Dosimetry for Total Skin Electron Therapy: Scintillator Target Imaging.* Int J Radiat Oncol Biol Phys, (2018).
[26] Garg, A.K., E.K. Frija, T.L. Sun, E.A. Strom, G.H. Perkins, J.J. Oh, T.K. Yu, W.A. Woodward, W.A. Tereffe, M. Sotirescue, and T.A. Buchholz, *Effects of variable placement of superior tangential/supraclavicular match line on dosimetric coverage of level III axilla/axillary apex in patients treated with breast and supraclavicular radiotherapy.* Int J Radiat Oncol Biol Phys, **71**(2): p. 370-4 (2009).
[27] Spraker, M.B., K. Fain, Jr., G. Goyan, J. Zong, M. Nyflot, L. Jordan, G. Kane, and E. Ford, *Evaluation of near-miss and adverse events in radiation oncology using a comprehensive causal factor taxonomy.* Pract Radiat Oncol, **7**(5): p. 346-353 (2017).
[28] Evans, S.B., *First Fruits of the RO-ILS system: Are we learning anything new?* Pract Radiat Oncol, **6**(2): p. 133-135 (2016).
[29] Hoopes, D.J., A.P. Disher, N.L. Eads, G.A. Ezzell, B.A. Fraass, T.M. Kwiatkowski, K. Lash, G.A. Patton, T. Piotrowski, C. Tomlinson, and E.C. Ford, *RO-ILS: Radiation Oncology Incident Learning System: A report from the first year of experience.* Pract Radiat Oncol, **5**(5): p. 312-318 (2015).
[30] Tendler, II, A. Hartford, M. Jermyn, E. Laflochelle, X. Cao, V. Borza, D. Alexander, P. Bruza, J. Hoopes, K. Moodie, B.P. Marr, B.B. Williams, B.W. Pogue, D.J. Gladstone, and L.A. Jarvis, *Experimentally Observed Cherenkov-Light Generation in the Eye During Radiotherapy.* Int J Radiat Oncol Biol Phys, (2018).

ACKNOWLEDGEMENTS

This work has been predominantly funded by NIH grant R01 EB023909 and supported by camera use and installation through R44 CA232879 and through the support of the Norris Cotton Cancer Center shared resources in P01 CA023108.

CONTACT INFORMATION

Prof. Brian Pogue, PhD
MacLean Professor of Engineering
Professor of Surgery, Geisel School of Medicine
Co-Director, Translational Engineering in Cancer Research Program, Norris Cotton Cancer Center
Brian.W.Pogue@dartmouth.edu
Office: (603) 646-3861

Rachael Hachadorian, MSc
PhD Candidate – Pogue Lab
Thayer School of Engineering
Dartmouth College
Rachael.L.Hachadorian.TH@dartmouth.edu
Lab: 603-650-1925
Cell: 858-243-8133

Lesley A. Jarvis, MD, PhD
Radiation Oncologist,
Dartmouth Hitchcock Medical Center
Associate Professor of Medicine, Geisel School of Medicine
Dartmouth College
Lesley.A.Jarvis@Hitchcock.org
Office: 603-650-6600